

# Calculating the Habitable Zone of Binary Star Systems II: P-Type Binaries

Nader Haghighipour<sup>1,2</sup> and Lisa Kaltenegger<sup>3,4</sup>

## ABSTRACT

We have developed a comprehensive methodology for calculating the circumbinary HZ in planet-hosting P-type binary star systems. We present a general formalism for determining the contribution of each star of the binary to the total flux received at the top of the atmosphere of an Earth-like planet, and use the Sun's HZ to calculate the inner and outer boundaries of the HZ around a binary star system. We apply our calculations to the *Kepler*'s currently known circumbinary planetary systems and show the combined stellar flux that determines the boundaries of their HZs. We also show that the HZ in P-type systems is dynamic and depending on the luminosity of the binary stars, their spectral types, and the binary eccentricity, its boundaries vary as the stars of the binary undergo their orbital motion. We present the details of our calculations and discuss the implications of the results.

*Subject headings:* Astrobiology: Habitable zone – Stars: binaries – Stars: Planetary systems – atmospheric effects

## 1. Introduction

The success of the Kepler space telescope in detecting planets in circumbinary orbits (also known as P-type systems) has opened a new chapter in the studies of planets in binary stars. Although the discovery of P-type planets had been previously announced around eclipsing binaries [e.g. the binaries NN Ser (Beuermann et al. 2010), UZ For (Potter et al. 2011), HU Aqu (Qian et al. 2011)] the orbital (in)stability of these objects cast doubt

---

<sup>1</sup>Institute for Astronomy and NASA Astrobiology Institute, University of Hawaii-Manoa, Honolulu, HI 96822

<sup>2</sup>Institute for Astronomy and Astrophysics, University of Tuebingen, 72076 Tuebingen, Germany

<sup>3</sup>MPIA, Koenigstuhl 17, Heidelberg, D 69117, Germany

<sup>4</sup>CfA, MS-20, 60 Garden Street, Cambridge, MA 02138, USA

on their validity (Wittenmyer et al. 2012; Hinse et al. 2012a,b; Goździewski et al. 2012). The confirmed detection of the seven currently known circumbinary planets, namely Kepler 16b (Doyle et al. 2011), Kepler 34b and Kepler 35b (Welsh et al. 2012), Kepler 38b (Orosz et al. 2012a), Kepler 47b&c (Orosz et al. 2012b), and Kepler 64b (Schwamb et al. 2013), however, has made it certain that planet formation *around* binary star systems is robust, and these systems may host planets of a variety of sizes including terrestrial size.

As the discovery of P-type planetary systems points to the viability of planet formation in circumbinary orbits, we address whether these systems can also provide habitable conditions. Similar to single stars, in order for a P-type system to host a rocky planet with habitable conditions, an Earth-like planet has to maintain a long-term stable orbit in the binary’s habitable zone (HZ). This implies that in order to assess the habitability of a P-type system, one has to first determine the location of its HZ. The latter is the focus of this paper. We follow our approach as presented in Kaltenegger & Haghighipour (2013, hereafter Paper I), and using the concept of *spectrally-weighted* flux, present a comprehensive methodology for calculating the locations of the inner and outer boundaries of the HZ in a circumbinary system.

Since the announcement of the circumbinary planet Kepler-16b, several efforts have been made to calculate the HZ of the currently known P-type systems. The first attempt was made by Quarles et al. (2012) who considered the system of Kepler 16 to be equivalent to a single star system for the purpose of calculating its HZ. Liu et al. (2013) also made an effort in calculating the HZ of Kepler 16 by adopting an equilibrium temperature approach that greatly diverges from the current model of HZ as developed by Kopparapu et al. (2013a). Similar approach has recently been taken by Mason et al. (2013) who have also calculated the HZ of currently known Kepler’s circumbinary planetary systems.

A common assumption in all these studies (which has led to their estimates of the HZ to be unreliable) has been that the equilibrium temperature on the surface of a fictitious Earth-like planet is due to the direct summation of the flux of each star of the binary in the planet’s orbit. In other words, the effect of the planet’s atmosphere and its response to the radiation from each star has been neglected. It is, however, known that the atmosphere of a planet plays an important role in its habitability. The planet’s atmosphere is the medium where the stellar radiation is first received and the process of converting from insolation to equilibrium temperature occurs. As stars with different spectral types have different spectral distributions of incident energy, the response of an atmosphere will be different for radiations from different stars. This implies that stars with different spectral energy distributions (SED) contribute differently to the energy absorbed at the top of the planet’s atmosphere (Kasting et al. 1993). In other words, a direct summation of the fluxes received

in the location of the planet is not applicable, and in order to obtain the total insulation received by the planet from the two stars of the binary, the flux of each star has to be weighted separately and according to its spectral type. The total flux received by the planet’s atmosphere will then be equal to the sum of the spectrally-weighted flux of each star (Paper I).

The fact that the direct summation of fluxes of the two stars of the binary cannot be used to determine the binary HZ have also been noted in a paper by Kane & Hinkel (2013). These authors used the limits of the narrow HZ without a cloud feedback [as calculated by Kasting et al. (1993), converted into flux limits by Underwood et al. (2003), and recently updated by Kopparapu et al. (2013b)], and determined the total flux at the location of the planet by adding the fluxes of the two stars. To avoid the above-mentioned short-comings, these authors treated each star as a black body, and defined an effective temperature that would allow for replacing the sum of the fluxes of the two stars by the flux from a single source with an equivalent energy. While this approach results in a more reliable determination of the binary HZ than those in the previously mentioned studies, the fact that the equivalent source of energy has been defined by using the direct summations of the fluxes of the two stars still does not allow for the effect of the SED of each star on the total flux absorbed by the planet’s atmosphere to be taken into account. As a result, this method, too, does not address the effect of the planet’s atmosphere. In this paper, we present a solution to this problem by introducing a comprehensive analytical approach to the calculation of the HZ in a circumbinary system which directly takes into account the contribution of each star due to its physical properties (including its SED), as well as its motion in the binary system.

To determine the location and range of the circumbinary HZ, similar to the calculations of HZ around single stars, we consider a fictitious Earth-like planet with a  $\text{CO}_2/\text{H}_2\text{O}/\text{N}_2$  atmosphere, and use the most recent model of Sun’s HZ developed by (Kopparapu et al. 2013a,b) to identify regions around the binary system where the total flux at the top of the planet’s atmosphere will be equal to that of the Earth at the inner and outer boundaries of the Sun’s HZ. Considering such an Earth analog in a P-type system is equivalent to assuming that Earth-like planets can in fact form in circumbinary orbits. Although at the time of the writing of this article, no Earth-like planets had been detected around binary stars, simulations of the last stage of the formation of terrestrial planets indicate that terrestrial-size object can in fact form and maintain stability in circumbinary orbits. We refer the reader to Haghighipour (2010) for a comprehensive review, in particular chapter 1 on potentially planet-forming circumbinary disks, and chapters 10 and 11 on the formation and stability of planets in P-type systems. In this study, we assume that despite some recent unsuccessful efforts in modeling the formation of P-type planets (Meschiari 2012), the detection of giant planets in P-type orbits is an indication that planet formation can proceed efficiently in

circumbinary disks, and Earth-like planets can form in orbits around a binary star system.

Figure 1 shows the orbit of a planet in a P-type system. As shown in the top panel of this figure, the two stars of the binary revolve around their center of mass (shown by CoM). In general, the orbit of the planet is around the center of mass of the entire three body system of Primary-Secondary-Planet. However, due to the negligible mass of the planet compared to those of the binary stars, the center of mass of the entire system is considered to be the same as the center of mass of the binary (CoM). Also, it is customary to assume that the primary is at rest and both the secondary and planet orbit a stationary primary (bottom panel of figure 1). As explained in the next section, in this paper we follow this convention.

It is important to note that the orbit of a planet in a P-type system, in addition to the inherent (in)stability associated with circumbinary orbits (i.e., the  $n : 1$  mean-motion resonances for  $3 < n < 9$ , Dvorak 1984, 1986; Dvorak et al. 1989; Holman & Wiegert 1999; Haghighipour 2010), is also driven by the extent of the circumbinary disk in which the planet is formed. As shown by Artymowicz & Lubow (1994), the interaction between the stars of a binary and the disk results in disk truncation and the removal of planet-forming material from the inner part of the disk. This effect is stronger in binaries with larger eccentricities causing the inner boundary of the disk and the stability limit to be slightly outside the influence zone of the binary stars. The latter implies that circumbinary planets can theoretically form around binaries with variety of eccentricities (a survey of the currently known P-type systems shows that the binary eccentricity can be as high as 0.52 in the case of Kepler 34). In binaries with high eccentricity, the close approach of the binary stars to a planet can change the flux contribution of each of the binary stars to the overall flux received by the planet, substantially. This effect combined with the response of the planet’s atmosphere to the radiation received from each star defines the HZ around the binary system. In this paper, we present a general methodology for calculating the boundaries of the HZ in a P-type system by taking the dynamical and physical characteristics of each star into account.

We describe our model and present the calculations of the HZ in Section 2. In section 3, we apply our methodology to the currently known P-type systems detected by the Kepler space telescope. Since the goal of our study is only to determine the location of the HZ, we do not consider the known planets in these systems. Instead we assume a fictitious Earth-like planet with a  $\text{CO}_2/\text{H}_2\text{O}/\text{N}_2$  atmosphere (Kasting et al. 1993, Selsis et al. 2007, and Kaltenegger & Sasselov 2011) in a circumbinary orbit around these binaries and determine the distances at which such a planet would both be dynamically stable and receive a combined stellar flux according to the flux in the HZ. In Section 4, we conclude this study by summarizing the results and discussing their implications.

## 2. Description of the Model and Calculation of HZ

### 2.1. Spectral Weight Factor

As mentioned in the Introduction, to determine the boundaries of the HZ, we adopt the same model and methodology as in Paper I. We consider a circumstellar HZ to be an annulus around a star where an Earth-like planet with a  $\text{CO}_2/\text{H}_2\text{O}/\text{N}_2$  atmosphere and sufficient amount of water can permanently maintain liquid water on its solid surface. We also assume that similar to Earth, geophysical cycles in this planet regulate the amount of its atmospheric  $\text{CO}_2$  and  $\text{H}_2\text{O}$ , and as a result, the locations of the inner and outer boundaries of its HZ will be associated with  $\text{CO}_2$ - and  $\text{H}_2\text{O}$ -dominated atmospheres, respectively. In such a planet, the concentration of atmospheric  $\text{CO}_2$  varies inversely with the surface temperature. In this paper, we adopt the model recently proposed by Kopparapu et al. (2013a,b) as the model for the Sun’s HZ without cloud feedback. In this model, a narrow HZ is defined as the region with an inner boundary at the Runaway Greenhouse limit, and an outer boundary at the distance where Earth will develop its Maximum Greenhouse effect. Note that the inner and outer boundaries of a narrow HZ are also without cloud feedback. We use the distances presented by these authors as Recent Venus and Early Mars for an empirical (nominal) HZ. These boundaries have been derived from the fluxes received by Mars at 3.5 Gy and by Venus at 1.0 Gy, at the time when both planets do not show indications for liquid water on their surfaces (Kasting et al. 1993).

The locations of the boundaries of the HZ and therefore, the capability of a planet in maintaining conditions for habitability depend on the total flux received at the top of the planet’s atmosphere. Since the atmosphere converts stellar insolation to temperature structure and surface temperature of a planet, its interaction with the stellar radiation plays an important role in considering if a planet can maintain liquid water on its surface and allow for detectable habitable conditions.

This interaction strongly depends on the stellar SED implying that stars with different energy distributions will contribute differently to the absolute incident flux at the top of the planet’s atmosphere. To determine the contribution of a star taking into account its SED, we define the quantity *spectral weight factor*  $W_i(f, T_i)$ , where  $i = (\text{Pr}, \text{Sec})$  denoting the primary and secondary stars, respectively,  $T_i$  is the star’s effective temperature, and  $f$  represents the atmosphere’s cloud fraction. As shown in Paper I and following Kopparapu et al. (2013a),

$$W_i(f, T_i) = \left[ 1 + \alpha_x(T_i) l_{x-\text{Sun}}^2 \right]^{-1}, \quad (1)$$

where

$$\alpha_x(T_i) = a_x T_i + b_x T_i^2 + c_x T_i^3 + d_x T_i^4. \quad (2)$$

In these equations,  $x=(\text{in},\text{out})$  denotes the inner and outer boundaries of the HZ,  $l_{x-\text{Sun}} = (l_{\text{in-Sun}}, l_{\text{out-Sun}})$  are in AU, and  $T_i(\text{K}) = T_{\text{Star}}(\text{K}) - 5780$ . The values of coefficients  $a_x, b_x, c_x$ , and  $d_x$  depend on the boundary of the Sun's HZ and are given in Table 1 (Kopparapu et al. 2013b). The graphs of the corresponding spectral weight factors of these models are shown in the top panel of figure 2.

## 2.2. Calculation of the Boundaries of Habitable Zone

Given the concept of spectral weight factor as introduced in the previous section, the contribution of each star of the binary to the total flux at the top of the planet's atmosphere can be written as  $W_i(f, T_i) F_i(f, T_i)$ . Here  $F_i = L_i/r_{\text{Pl}-i}^2$  denotes the stellar flux and  $L_i$  is the luminosity of each star of the binary. The total flux received by the planet is, therefore, given by

$$W_{\text{Pr}}(f, T_{\text{Pr}}) \frac{L_{\text{Pr}}(T_{\text{Pr}})}{r_{\text{Pl-Pr}}^2} + W_{\text{Sec}}(f, T_{\text{Sec}}) \frac{L_{\text{Sec}}(T_{\text{Sec}})}{r_{\text{Pl-Sec}}^2}, \quad (3)$$

where  $r_{\text{Pl-Pr}}$  and  $r_{\text{Pl-Sec}}$  are the distances between the planet and the primary and secondary stars, respectively. Defining HZ as a region where the total flux received by an Earth-like planet at that top of its atmosphere is equal to that of Earth received from the Sun, the boundaries of the HZ of the binary can be calculated from

$$W_{\text{Pr}}(f, T_{\text{Pr}}) \frac{L_{\text{Pr}}(T_{\text{Pr}})}{l_{x-\text{Bin}}^2} + W_{\text{Sec}}(f, T_{\text{Sec}}) \frac{L_{\text{Sec}}(T_{\text{Sec}})}{r_{\text{Pl-Sec}}^2} = \frac{L_{\text{Sun}}}{l_{x-\text{Sun}}^2}. \quad (4)$$

In deriving this equation, we have assumed that the primary star is at the center of the coordinates system (see the lower panel of figure 1) and the boundaries of the HZ of the binary ( $l_{x-\text{Bin}}$ ) are measured with respect to this star.

As shown by equation (4), calculations of the boundaries of HZ require calculating the distance between the secondary star and the Earth-like planet ( $r_{\text{Pl-Sec}}$ ). As shown by the bottom panel of figure 1, this quantity can be written as

$$r_{\text{Pl-Sec}}^2 = r_{\text{Pl-Pr}}^2 + r_{\text{Bin}}^2 - 2 r_{\text{Pl-Pr}} r_{\text{Bin}} \cos(\nu - \theta), \quad (5)$$

where  $\nu$  is the true anomaly of the binary,  $r_{\text{Bin}} = a_{\text{Bin}}(1 - e_{\text{Bin}}^2)/1 + e_{\text{Bin}} \cos \nu$ , and  $r_{\text{Pl-Pr}} = l_{\text{x-Bin}}$ . In a circumbinary system, where the planet is subject to the gravitational forces of two stars, the angle  $\theta$  can be calculated using planet's equation of motion. Recently, Leung & Lee (2013) have presented an elegant analytical treatment of the orbit of a planet in a P-type system. While the methodology and solutions presented by these authors can be used to calculate  $\theta$ , we present here an approach that is more efficient when used in numerical computations.

In general, the equation of motion of a planet in a circumbinary orbit, as shown in the lower panel of figure 1, can be written as

$$\frac{d^2}{dt^2} \mathbf{r}_{\text{Pl-Pr}} = -G \frac{M_{\text{Pr}}}{r_{\text{Pl-Pr}}^3} \mathbf{r}_{\text{Pl-Pr}} - G \frac{M_{\text{Sec}}}{r_{\text{Pl-Sec}}^3} \mathbf{r}_{\text{Pl-Sec}}. \quad (6)$$

In equation (6),  $\mathbf{r}_{\text{Pl-}i}$  are the vectors connecting the planet to the binary stars,  $M_i$  represents stellar masses, and  $G$  is the gravitational constant. Considering a plane-polar coordinates system (which would be consistent with the co-planarity of Kepler circumbinary planets), equation (6) can be written as

$$P_r = \dot{r}, \quad (7)$$

$$P_\theta = r^2 \dot{\theta}, \quad (8)$$

$$\dot{P}_r = \frac{\dot{P}_\theta}{r^3} - \frac{1}{r^2} - \frac{\varepsilon}{|\mathbf{r} - \mathbf{r}_{\text{Bin}}|^3} \left[ r - r_{\text{Bin}} \cos(\nu - \theta) \right], \quad (9)$$

$$\dot{P}_\theta = -\varepsilon \frac{r r_{\text{Bin}}}{|\mathbf{r} - \mathbf{r}_{\text{Bin}}|^3} \sin(\nu - \theta). \quad (10)$$

where  $\mathbf{r} = \mathbf{r}_{\text{Pl-Pr}}$ ,  $\varepsilon = M_{\text{Sec}}/M_{\text{Pr}}$ , and we have set  $GM_{\text{Pr}} = 1$ . The boundaries of the HZ of the binary can be calculated by simultaneously solving equations (4) and (7-10), substituting for  $r_{\text{pl-Sec}}$  from equation (5).

### 2.3. Effect of Binary Eccentricity

The solutions of equations (4) and (7-10) present the actual motion of a planet in a circumbinary orbit. In the context of calculating the binary's HZ, the latter means, unlike



the usual practice of constraining the orbit of the fictitious Earth-like planet to a circle, the orbit of this planet will be affected by the dynamics of the binary and may not stay circular. As a result, as shown in the next section, depending on the contribution of each star and the binary eccentricity, the shape of the (instantaneous) HZ may also deviate from a circle and may vary during the motion of the binary.

The binary eccentricity will also play an important role in the formation and stability of the planet. As shown by Artymowicz & Lubow (1994), the interaction between the binary and a disk of circumbinary objects causes the disk to be truncated and lose some of its planet-forming material. As a result of the disk truncation, the inner edge of the disk will move out to the location of the boundary of the stability given by (Dvorak 1986; Dvorak et al. 1989; Holman & Wiegert 1999)

$$a_{\text{Min}} = a_{\text{Bin}} (1.60 + 5.10 e_{\text{Bin}} + 4.12 \mu - 2.22 e_{\text{Bin}}^2 - 4.27 \mu e_{\text{Bin}} - 5.09 \mu^2 + 4.61 \mu^2 e_{\text{Bin}}^2). \quad (11)$$

In this equation,  $\mu$  is the binary mass-ratio and is equal to  $M_{\text{Sec}}/(M_{\text{Pr}} + M_{\text{Sec}})$ . As shown by equation (11), the location of the stability region is strongly affected by the eccentricity of the binary. In binaries with large eccentricities, this region moves to large distances implying that (depending on the spectral types of the stars of the binary) the system may not be able to form potentially habitable planets. One can use equation (11) to determine the range of the binary eccentricity for which a planet in the HZ of the binary will be stable. For instance in the case of the narrow HZ, for a binary with a given mass-ratio  $\mu$ , the lower (upper) limit of the eccentricity corresponds to a value for which the boundary of stability coincides with the inner (outer) edge of the HZ.

### 3. Habitable Zones of the Kepler P-type systems

In this section, we calculate the boundaries of narrow and empirical HZs of the currently known Kepler circumbinary planetary systems. Using the model by Kopparapu et al. (2013a,b), we consider the narrow HZ (without cloud feedback) of a Sun-like star to extend from 0.97 AU to 1.67 AU, and its empirical HZ to be from 0.75 AU to 1.77 AU.

For each planetary system studied, we have created movies of the time evolution of the HZ. These movies can be downloaded from <http://astro.twam.info/hz-ptype/>. In the following, we will show snapshots of some of these movies for a subset of the calculations for each system. In each snapshot, the dark green represents the narrow HZ and the light green corresponds to the empirical HZ. We also show the orbits of the currently known planets of



each system (in blue) and the boundary of the planetary stability (in red).

### 3.1. Kepler 16

The Kepler 16 binary system (Doyle et al. 2011) consist of a 0.69 solar-mass ( $M_\odot$ ) primary with a radius of 0.65 solar-radii ( $R_\odot$ ) and an effective temperature of 4450 K. The secondary of this system is an M dwarf with a mass of  $0.20M_\odot$  and radius of  $0.23R_\odot$ . The binary semimajor axis in this system is 0.22 AU, and its eccentricity is 0.16. We calculated the luminosity of the primary star using

$$\frac{L_*}{L_\odot} = \left( \frac{R_*}{R_\odot} \right)^2 \left( \frac{T_*}{T_\odot} \right)^4, \quad (12)$$

where  $L_*$ ,  $R_*$ , and  $T_*$  represent the stellar luminosity, radius, and effective temperature, respectively. Using  $T_\odot = 5780$  K as the Sun’s effective temperature, the luminosity of Kepler 16A is equal to  $0.148L_\odot$ . To calculate the luminosity of the secondary star, we used the mass-luminosity relation  $L \sim 0.23 M_*^{2.3}$  where  $M_*$  is the mass of the star (Duric 2004). From this relationship, the secondary has a luminosity of  $0.0057L_\odot$  which combined with equation (12) results in an effective temperature of  $\sim 3311$  K for this star.

Table 2 shows the values of the spectral weight factors of the stars of Kepler 16 binary system and boundaries of its HZ. As shown here, the outer boundaries of the narrow and empirical HZs are larger than 0.7 AU. As a point of comparison, the semimajor axis of the currently known circumbinary planet of this system is  $\sim 0.705$  AU (Doyle et al. 2011) and the limit of its planetary orbit stability (i.e., the distance beyond which the orbit of a circumbinary planet will be stable) obtained from equation (11), is at 0.63 AU. Given the almost circular orbit of this planet ( $e \sim 0.007$ ), this implies that the giant planet of this system has a long-term stable orbit close to the outer edge of its HZ.

To determine to what extent the motion of the secondary star affects the location of the HZ, we calculated the narrow and empirical HZs of the system for one complete orbital motion of the secondary. Movies of the time-dependent locations of these HZs can be found at <http://astro.twam.info/hz-ptype/>. As an example, we show in figure 3 four snapshots of the evolution of the HZ for one orbit of the binary. The left column in this figure shows a top view of the HZ, and the right column shows the changes in the locations of the boundaries of the HZ. From top to bottom, the panels correspond to the true anomaly of the secondary equal to 0, 60°, 120° and 180°, respectively. As shown here, both the inner and outer boundaries of the HZ extend slightly outward at closest distances to the secondary star.

Figure 3 also shows (in red) the boundary of the stability of planetary orbits around the binary and (in blue) the orbit of the currently known planet of this system. As shown here, a large portion of the HZ of the Kepler 16 is interior to its critical distance indicating that the most of the HZ of this system is unstable.

### 3.2. Kepler 34

The eclipsing binary Kepler 34 consists of two Sun-like stars. The primary of this system has a mass of  $1.048 M_{\odot}$  with a bolometric luminosity of  $1.49 L_{\odot}$  and an effective temperature of 5913 K. The mass of the secondary star is  $1.021 M_{\odot}$ , its bolometric luminosity is 1.28 solar, and it has an effective temperature of 5867 K (Welsh et al. 2012). The semimajor axis of this binary is  $\sim 0.23$  AU and it has an eccentricity of  $\sim 0.521$ , making Kepler 34 the most eccentric planet-hosting binary star system known to date (Welsh et al. 2012). Table 3 shows the spectral weight factors for the primary and secondary stars, and the locations of the inner and outer boundaries of the binary’s HZ. As expected, because the stars of this binary are Sun-like, the distance of the HZ to the primary star is much larger than the stellar separation. However, due to the large binary eccentricity in this system, the effect of the orbital motion of the secondary on the locations of the boundaries of the HZ, although smaller than that in Kepler 16, is still noticeable. Figure 4 shows this for the narrow and empirical HZs, and for the same values of the true anomaly as in figure 3. The changes in the locations of the boundaries of the binary HZ over the binary’s full orbit can be seen more clearly in the right panels. Figure 4 also shows the boundary of the orbital stability around Kepler 34 (at  $\sim 0.84$  AU) and the orbit of its currently known planet. As shown here, the combination of the small semimajor of the binary and that its stars are of solar type has placed the entire HZ of this system in the stable region. As shown in Table 3, only when the empirical HZ is considered, the circumbinary planet of Kepler 34, with a semimajor axis of 1.089 AU and eccentricity of 0.18 (Welsh et al. 2012) spends a small portion of its orbit in the binary’s empirical HZ.

### 3.3. Kepler 35

The Kepler 35 system is an (almost) equal-mass binary with a  $0.89M_{\odot}$  primary and a secondary star with a mass of  $0.81M_{\odot}$ . The bolometric luminosity of the primary of this system is  $0.94L_{\odot}$  and it has an effective temperature of 5606 K. The secondary star in this system has a bolometric luminosity of  $0.41L_{\odot}$  and its effective temperature is 5202 (Welsh et al. 2012). The semimajor axis of the Kepler 35 binary is  $\sim 0.18$  AU and its

eccentricity is 0.14. Table 4 shows the spectral weight factors and the distances of the inner and outer boundaries of the HZ of this binary system. Similar to the case of Kepler 34, the HZ of Kepler 35 is at distances much larger than the separation of its two stars. This, combined with the small eccentricity of this binary has caused the effect of the orbital motion of its secondary on the displacement of the inner and outer boundaries of its HZ to be small. Figure 5 shows this in more detail. In this figure, the narrow and empirical HZs of the system are shown when the secondary star is at its perihelion and aphelion distances. Figure 5 also shows that as in the system of Kepler 34, the stability limit for circumbinary planetary orbits is at a much closer distance ( $\sim 0.51$  AU) indicating that planets in the HZ of Kepler 35 will have stable orbits. The circumbinary planet of this system, with its semimajor axis equal to 0.6 AU and its eccentricity equal to 0.04 (Welsh et al. 2012), however, although stable, is not in the binary HZ.

### 3.4. Kepler 38

The binary star Kepler 38 consists of a moderately evolved  $0.95M_{\odot}$  star as its primary and a low-mass ( $0.25M_{\odot}$ ) stellar companion in an approximately 18.8 day orbit as its secondary. The semimajor axis of the binary is  $\sim 0.15$  AU, and its eccentricity is 0.10 (Orosz et al. 2012a). Using equation (12) and the values of the radius ( $\sim 1.76R_{\odot}$ ) and effective temperature (5623 K) of the primary as reported by Orosz et al. (2012a), the luminosity of this star is approximately equal to  $2.77L_{\odot}$ . We calculated the luminosity of the secondary star in a similar way, using the value of its radius ( $0.27R_{\odot}$ ) and the ratio of its effective temperature to that of the primary (0.59) as given by Orosz et al. (2012a). As expected, this star has a much smaller luminosity, equal to  $0.008L_{\odot}$ . Table 5 shows the values of the spectral weight factors and the boundaries of the HZ of this system. Given the significantly smaller luminosity of the secondary star, the location and width of the HZ around this binary are mainly due to the radiation from the primary star. As shown in figure 6, the orbital motion of the secondary does not cause noticeable changes in the inner and outer boundaries of its narrow and empirical HZs. The stability limit of the Kepler 38 binary is at 0.40 AU implying that the HZ of this system is in the stable region. However, the orbit of the currently known circumbinary planet of this system is entirely interior to the inner boundary of its HZ.

### 3.5. Kepler 47

The binary system of Kepler 47 is a unique case study in the sense that it presents the first binary system with multiple planetary companions (Orosz et al. 2012b). The primary of this system is a solar-mass star ( $1.043M_{\odot}$ ) with a radius of  $0.964R_{\odot}$ , effective temperature of 5636 K, and luminosity of  $0.84L_{\odot}$ . The secondary of this system is a 0.362 solar-mass M star with a radius, effective temperature and luminosity of  $0.3506R_{\odot}$ , 3357 K, and  $0.014L_{\odot}$ , respectively (Orosz et al. 2012b). The orbit of the binary is almost circular ( $e_{\text{Bin}} = 0.02$ ) and its semimajor axis is approximately 0.08 AU. Kepler 47 is host to two Neptune-sized planets b and c with semimajor axes of 0.29 AU and 0.99 AU, respectively (Orosz et al. 2012b).

Table 7 shows the values of the spectral weight factors and boundaries of the HZ of the system. Our calculations indicate that similar to the case of Kepler 38, the HZ of this system is primarily due to the insolation received from the primary star, and the effect of the secondary, although larger than that of Kepler 38, is still negligible. Figure 7 shows the narrow and empirical HZs of this system, and the boundary of planetary stability at 0.19 AU. As shown here, the HZ of the system is dynamically stable. Figure 7 and Table 7 also show that the outer boundaries of the narrow and empirical HZs of the system are slightly larger than 1.5 AU indicating that the majority of the orbit of planet c in this system is in the HZ. We would like to note that while being a Neptune-sized planet, Kepler 47c cannot be habitable. However, it may harbor terrestrial-class habitable moons and Trojan planets that may be able to develop and sustain conditions for habitability (see, for instance, Kaltenegger 2010; Haghighipour et al 2013, and references therein).

### 3.6. Kepler 64

Kepler 64 is an F-M binary with a semimajor axis of  $\sim 0.17$  AU and eccentricity of  $\sim 0.21$ . The primary of this system (F star) has a mass of  $1.528M_{\odot}$ , radius of  $1.734R_{\odot}$ , and an effective temperature of 6407 K (Schwamb et al 2012). The mass of the secondary star is  $0.408M_{\odot}$ , its radius is  $0.378R_{\odot}$ , and it has an effective temperature of 3561 K (Schwamb et al. 2012). From these quantities and using equation (12), the luminosities of the primary and secondary stars of this system are  $4.54L_{\odot}$  and  $0.02L_{\odot}$ , respectively. These luminosities indicate that the primary of Kepler 64 will be the dominating star in calculating the location of the binary’s HZ. Table 8 and figure 8 show the values of the spectral weight factors and the boundaries of the narrow as well as empirical HZs for this system. As shown here, the orbital motion of the secondary does not have noticeable effects on the location of the HZ. Figure 8 also shows the critical distance for the orbital stability (at 0.52 AU) which indicates

that the HZ of Kepler 64 system is entirely stable. A comparison between the locations of the boundaries of the HZ in this system and the orbit of its circumbinary planet (semimajor axis of 0.63 AU and eccentricity of 0.05) shows that the HZ of Kepler 64 is much farther out than the orbit of its currently known planet.

#### 4. Summary and Concluding Remarks

We have developed a comprehensive methodology for calculating the boundaries of the circumbinary HZ of binary star systems. We used the concept of spectral weight factor, as defined in our calculations of the HZ in S-type binary systems (Kaltenegger & Haghighipour 2013), and determined the contribution of each star to the total flux received at the top of a fictitious circumbinary Earth-like planet. By comparing the insolation received by this planet with that received by Earth from the Sun, we determined the locations of the inner and outer boundaries of narrow and empirical HZs. Our calculations indicated that depending on the stellar type and orbital elements of the binary, the HZ may be dynamic, and the instantaneous locations of its inner and outer boundaries may change during the orbital motion of the binary. It is, however, important to note that the habitability of an Earth-like planet in a circumbinary HZ is independent of the fluctuations of the boundaries of the HZ. In this case, the determining factor is the averaged flux received by the planet in one orbit around the binary. During this time, the buffering effect of clouds should compensate for the effects of the temporary displacements of the HZ, and allow the planet to maintain a surface temperature conducive to liquid water.

To calculate the locations of the boundaries of the HZ, we used the limits of the Sun’s HZ as given by the model by Kopparapu et al. (2013a,b). This model presents the most up-to-date values for the boundaries of the Sun’s narrow HZ without cloud feedback. To account for the feedback of cloud, which extend the boundaries of the narrow HZ, we use as a second limit, the empirical HZ corresponding to the flux received by Venus and Mars for the time when we do not have indications for liquid water on the surfaces of these planets (Kasting et al. 1993). However, our methodology is general and can be applied to any model of the HZ including models with clouds, as they become available.

In conclusion, we would like to note that in order for a binary star to have a habitable circumbinary planet, an Earth-like object has to form and maintain a long-term stable orbit in its circumbinary HZ. The discovery of the currently known P-type systems lends strong support to the fact that planet formation can start and efficiently continue in circumbinary orbits. Simulations of the final stage of terrestrial planet formation have shown that subsequent to the disk truncation, planetesimals and protoplanetary bodies can successfully grow

to terrestrial-class objects and reside in long-term stable orbits. In binaries whose eccentricities allow the HZ to be stable, terrestrial/Earth-like planet formation proceeds similar to planet formation around single stars.

We are grateful to Tobias Müller at the Computational Physics group at the Institute for Astronomy and Astrophysics, University of Tübingen for making the movies and graphs of HZ. N.H. acknowledges support from the NASA Astrobiology institute under Cooperative Agreement NNA09DA77 at the Institute for Astronomy, University of Hawaii, HST grant HST-GO-12548.06-A, and Alexander von Humboldt Foundation. Support for program HST-GO-12548.06-A was provided by NASA through a grant from the Space Telescope Science Institute, which is operated by the Association of Universities for Research in Astronomy, Incorporated, under NASA contract NAS5-26555. N.H. is also thankful to the Computational Physics group at the Institute for Astronomy and Astrophysics, University of Tübingen for their kind hospitality during the course of this project. L.K. acknowledges support from NAI and DFG funding ENP Ka 3142/1-1.

## REFERENCES

- Artymowicz, P. & Lubow, S. H. 1994, *ApJ*, 421, 651
- Beuermann, K., et al., 2010, *A&A*, 521, L60
- Doyle, L. R., et al., 2011, *Science*, 333, 1602
- Duric, N., 2004, Book: *Advanced Astrophysics*, (Cambridge University Press, Cambridge, UK), pp. 19
- Dvorak, R., 1984, *Celest. Mech.*, 34, 369
- Dvorak, R., 1986, *A&A*, 167, 379
- Dvorak, R., Froeschle, C. & Froeschle, Ch., 1989, *A&A*, 226, 335
- Goździewski, K. et al., 2012, *MNRAS*, 425, 930
- Haghighipour, N., 2010, Book: *Planets in Binary Star Systems*, (Springer, New York)
- Haghighipour, N., Capen, S. & Hinse, T. C., 2013, *CeMDA*, in press
- Hinse, T. C., Goździewski, K., Lee, J. W., Haghighipour, N., & Lee, C-U., 2012, *AJ*, 144, article id. 34

- Hinse, T. C., Lee, J. W., Goździewski, K., Haghighipour, N., Lee, C-U., & Scullion, E. M., 2012, MNRAS, 420, 3609
- Holman M. J. & Wiegert P. A. 1999, AJ, 117, 621
- Kaltenegger, L. & Haghighipour, N., 2013, ApJ, in press
- Kaltenegger, L. & Sasselov, D. 2011, ApJL 736, article id. L25
- Kaltenegger, L., 2010, ApJ, 711, L1-L6
- Kane, S. R. & Hinkel, N. R., 2013, ApJ, 762, article id. 7
- Kasting, J. F., Whitmire, D. P. & Reynolds, R. T., 1993, Icarus, 101, 108
- Kopparapu, R. K., et al., 2013, ApJ, 765, article id. 131
- Kopparapu, R. K., et al. 2013, ApJ, 770, article id. 82
- Leung, G. C. K. & Hoi Lee, M., 2013, 763, article id. 107
- Liu, H-G., Zhang, H. & Zhou, J-L., 2013, ApJ, 767, L38
- Mason, P. A., Zuluaga, J. I., Clark, J. M. & Cuartas-restrepo, P. A. 2013, ArXiv: 1307.4624
- Meschiari, S., 2012, ApJ, 761, article id. L7
- Orosz J. A., et al. 2012a, ApJ, 758, article id. 87
- Orosz J. A., et al. 2012b, Science, 337, 1511
- Potter, S. B., et al., 2011, MNRAS, 416, 2202
- Qian, S-B., Liu, L., Liao, W.-P., Li, L.-J., Zhu, L.-Y., Dai, Z.-B., He, J.-J., Zhao, E.-G., Zhang, J. & Li, K., 2011, MNRAS, 414, L16
- Quarles, B., Musielak, Z. E. & Cuntz, M., 2012, ApJ, 750, article id. 14
- Schwamb, M. E., et al., 2013, ApJ, in press (arXiv:1210.3612)
- Selsis, F., Kasting, J. F., Levrard, B., Paillet, J., Ribas, I., Delfosse, X., A&A, 476, 1373
- Underwood, D. R., Jones, B. W. & Sleep, P. N. 2003, IJA, 2, 289
- Welsh, W. F., et al., 2012, Nature, 481, 475



Wittenmyer, R. A., Horner, J. A., Marshall, J. P., Butters, O. W., & Tinney, C. G., 2012,  
MNRAS, 419, 3258

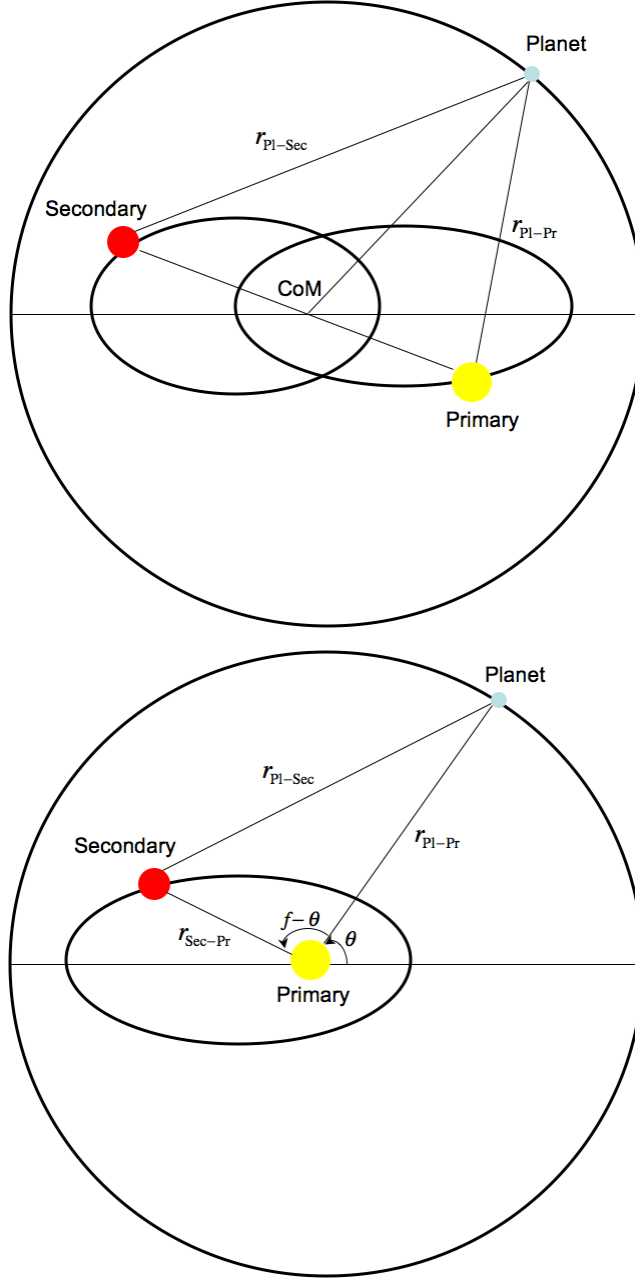


Fig. 1.— General schematic presentation of a P-type system. The top panel shows the general orbital configuration of the planet and the binary stars. Both stars and the planet rotate around the center of mass of the binary (shown by CoM). However, it is customary to consider the primary star to be stationary and both the secondary and planet rotates around this stars (bottom panel).

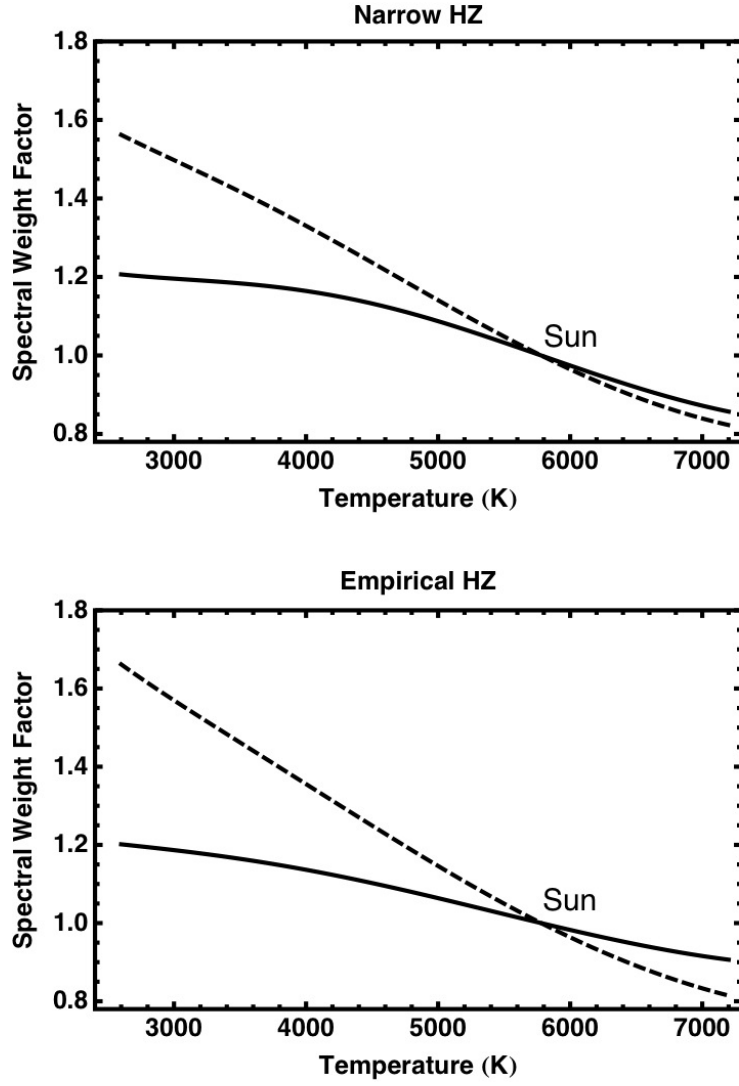


Fig. 2.— Graphs of the spectral weight factor in narrow and empirical HZs for different values of effective stellar temperature. The solid curves correspond to the inner boundaries of the HZ (Runaway Greenhouse in the case of narrow, and Recent Venus in the case of empirical HZs) and the dashed curves are for the outer boundaries (Maximum Greenhouse in the case of narrow, and Early Mars in the case of empirical HZs).

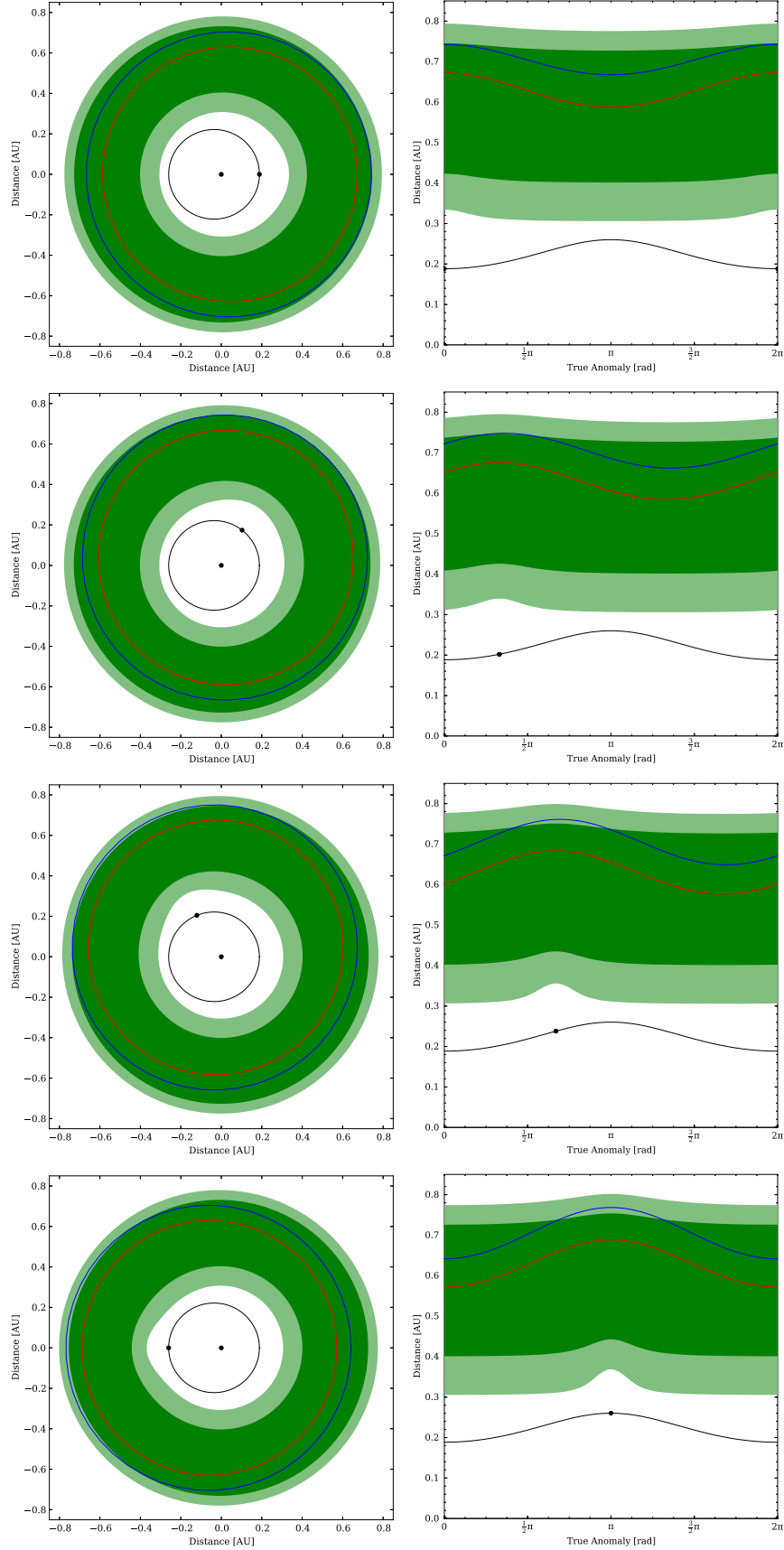


Fig. 3.— Snapshots of the radial variations of the narrow (dark Green, here and next figures) and empirical (light green, here and next figures) HZ around the Kepler 16 binary system. The snapshots are taken at 6 months intervals, starting from the epoch of the first observation.

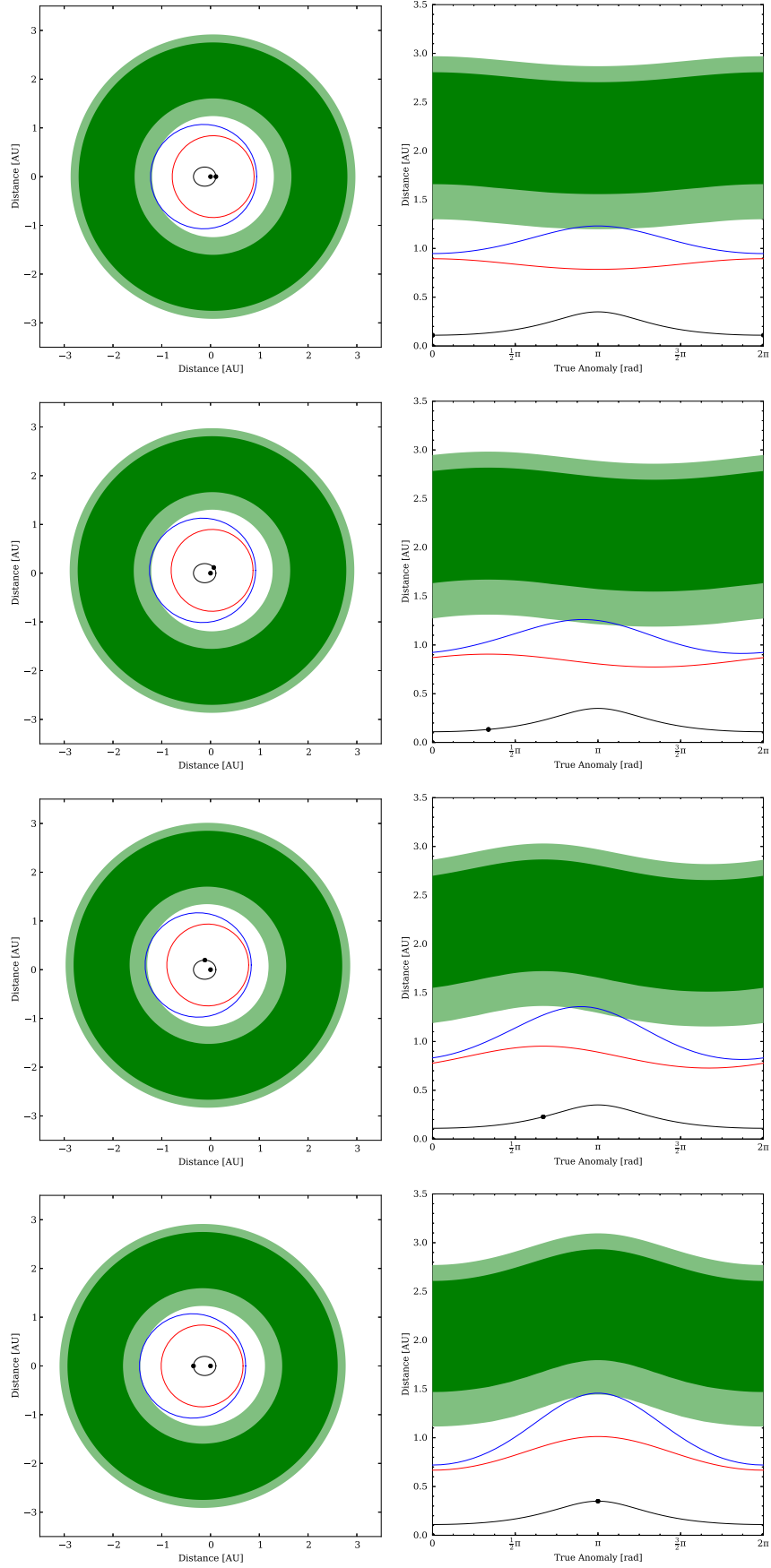


Fig. 4.— Graphs of the narrow and empirical HZ of Kepler 34 binary system.

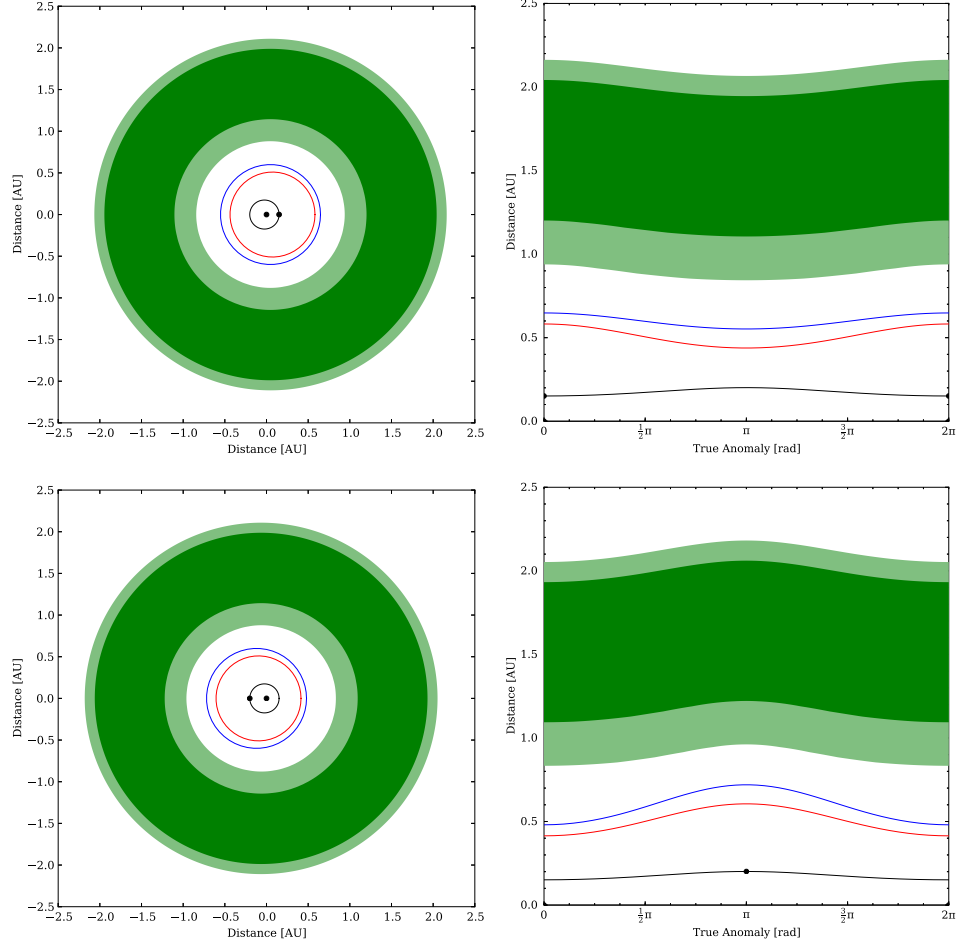


Fig. 5.— Graphs of the narrow and empirical HZ of Kepler 35 binary system. The right panels show the maximum and minimum radial variations in the boundaries of the HZ due to the orbital motion of the secondary.

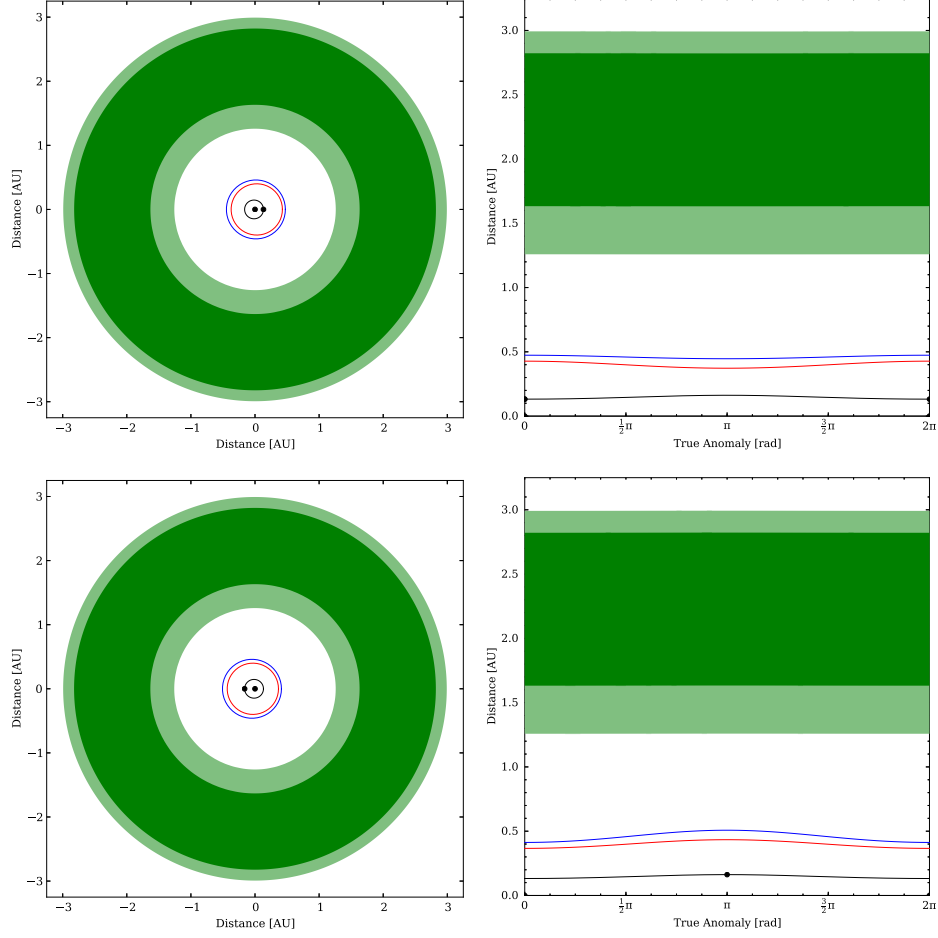


Fig. 6.— Graphs of the narrow and empirical HZ of Kepler 38 binary system. The right panels show the maximum and minimum radial variations in the boundaries of the HZ due to the orbital motion of the secondary. As shown here, the effect of the secondary star is negligible, and the location of the HZ is mainly determined by the primary star.



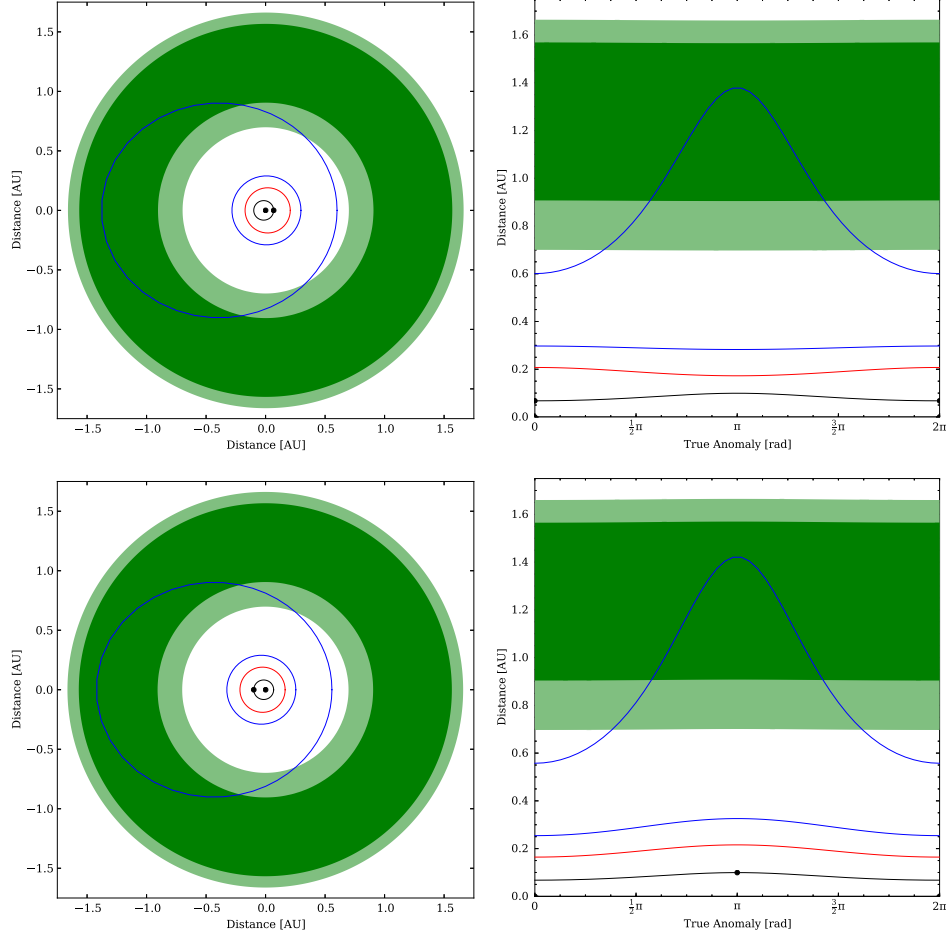


Fig. 7.— Graphs of the narrow and empirical HZ of Kepler 47 binary system. The right panels show the maximum and minimum radial variations in the boundaries of the HZ due to the orbital motion of the secondary. As shown here, the effect of the secondary star is minute indicating that the HZ of the system is in most part determined by the primary star. The figure also shows the orbits of the two planets of this system.

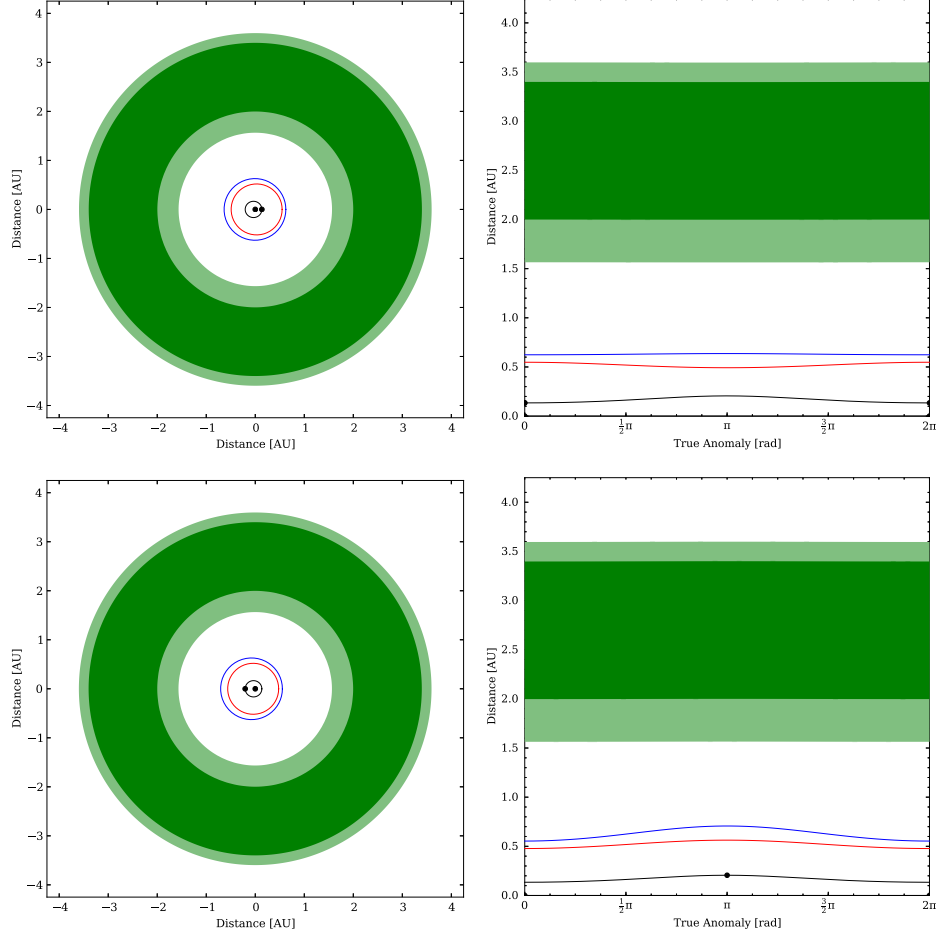


Fig. 8.— Graphs of the narrow HZ of Kepler 64 binary system. The right panels show the maximum and minimum radial variations in the boundaries of the HZ due to the orbital motion of the secondary. As shown here, the effect of the secondary star is negligible, and the location of the HZ is determined by the primary star.

Table 1. Values of the coefficients of equation (2) from Kopparapu et al. (2013b).

	Narrow HZ		Empirical HZ	
	Runaway Greenhouse	Maximum Greenhouse	Recent Venus	Early Mars
$l_{\text{x-Sun}}$ (AU)	0.97	1.67	0.75	1.77
Flux (Solar Flux @ Earth)	1.06	0.36	1.78	0.32
a	$1.2456 \times 10^{-4}$	$5.9578 \times 10^{-5}$	$1.4335 \times 10^{-4}$	$5.4471 \times 10^{-5}$
b	$1.4612 \times 10^{-8}$	$1.6707 \times 10^{-9}$	$3.3954 \times 10^{-9}$	$1.5275 \times 10^{-9}$
c	$-7.6345 \times 10^{-12}$	$-3.0058 \times 10^{-12}$	$-7.6364 \times 10^{-12}$	$-2.1709 \times 10^{-12}$
d	$-1.7511 \times 10^{-15}$	$-5.1925 \times 10^{-16}$	$-1.1950 \times 10^{-15}$	$-3.8282 \times 10^{-16}$

Table 2. Kepler 16

	Narrow HZ		Empirical HZ	
	inner	outer	inner	outer
Spectral Weight Factor (Primary)	1.136	1.246	1.106	1.260
Spectral Weight Factor (Secondary)	1.189	1.448	1.173	1.502
Boundaries of HZ (AU)	0.400	0.757	0.305	0.805

Table 3. Kepler 34

	Narrow HZ		Empirical HZ	
	inner	outer	inner	outer
Spectral Weight Factor (Primary)	0.984	0.978	0.989	0.978
Spectral Weight Factor (Secondary)	0.990	0.986	0.993	0.985
Boundaries of HZ (AU)	1.506	2.853	1.147	3.018

Table 4. Kepler 35

	Narrow HZ		Empirical HZ	
	inner	outer	inner	outer
Spectral Weight Factor (Primary)	1.020	1.029	1.014	1.030
Spectral Weight Factor (Secondary)	1.066	1.102	1.047	1.106
Boundaries of HZ (AU)	1.092	2.097	0.831	2.184

Table 5. Kepler 38

	Narrow HZ		Empirical HZ	
	inner	outer	inner	outer
Spectral Weight Factor (Primary)	1.018	1.027	1.013	1.027
Spectral Weight Factor (Secondary)	1.188	1.447	1.173	1.501
Boundaries of HZ (AU)	1.631	2.823	1.258	2.992

Table 6. Kepler 47

	Narrow HZ		Empirical HZ	
	inner	outer	inner	outer
Spectral Weight Factor (Primary)	1.017	1.024	1.012	1.025
Spectral Weight Factor (Secondary)	1.187	1.441	1.171	1.492
Boundaries of HZ (AU)	0.904	1.569	0.697	1.664

Table 7. Kepler 64

	Narrow HZ		Empirical HZ	
	inner	outer	inner	outer
Spectral Weight Factor (Primary)	0.929	0.906	0.952	0.903
Spectral Weight Factor (Secondary)	1.182	1.407	1.161	1.449
Boundaries of HZ (AU)	1.997	3.400	1.562	3.598